Available online at www.sciencedirect.com
SCIENCE DIRECT®
Journal of Nuclear Materials 329–333 (2004) 1243–1247
journal of nuclear materials
www.elsevier.com/locate/jnucmat

A master curve analysis of F82H using statistical and constraint loss size adjustments of small specimen data

G.R. Odette [a,*], T. Yamamoto [a], H. Kishimoto [a], M. Sokolov [b], P. Spätig [a,c], W.J. Yang [a], J.-W. Rensman [d], G.E. Lucas [a]

[a] Department of Mechanical and Environmental and Engineering, University of California, Santa Barbara, CA 93106-5070, USA
[b] Oak Ridge National Laboratory, USA
[c] CRPP EPFL, Switzerland
[d] NRG Petten, The Netherlands

Abstract

We assembled a fracture toughness database for the IEA heat of F82H based on a variety of specimen sizes with a nominal ASTM E1921 master curve (MC) reference temperature $T_0 = -119 \pm 3$ °C. However, the data are not well represented by a MC. T_0 decreases systematically with a decreasing deformation limit $M_{\lim}$ starting at ≈200, which is much higher than the E1921 censoring limit of 30, indicating large constraint loss in small specimens. The small scale yielding T_0 at high $M_{\lim}$ is $\approx 98 \pm 5$ °C. While, the scatter was somewhat larger than predicted, after model-based adjustments for the effects of constraint loss, the data are in reasonably good agreement with a MC with $T_0 = -98$ °C. This supports to use of MC methods to characterize irradiation embrittlement, as long as both constraint loss and statistical size effects are properly accounted for. Finally, we note various issues, including sources of the possible excess scatter, which remain to be fully assessed.

1. Introduction

One of the key challenges facing the development of ≈8Cr normalized and tempered martensitic steels (TMS) for fusion applications is irradiation embrittlement. Embrittlement is best characterized in terms of fracture toughness–temperature curves, $K_{Jc}(T)$. Measuring fracture toughness requires pre-cracked specimens subject to strict size and geometry requirements. Various versions of the master curve (MC) method, described in the next section [1–4], greatly reduce fracture toughness testing requirements in terms of both the size and number of specimens. This is critical since embrittlement depends on the combination of a large number of variables and there are very severe restrictions on irradiation volumes that can be accessed, particularly at high dose and with good control of specimen temperatures.

However, use of small specimens demands that the issue of size effects be addressed directly [1,3,5–11]. The sources of such size effects and approaches to accounting for them are described in the next section. We focus on the issue of determining a toughness temperature curve, $K_{Jr}(T)$, for the IEA F82H reference heat. Previous studies suggested that there was considerable variability in the $K_{Jr}(T)$ data for this heat, presumably associated with heterogeneities in the underlying microstructure, suggesting that a single MC can not represent IEA F82H. However, size effects were not fully assessed in the previous studies, confounding this conclusion. In order to evaluate the applicability of the MC method to TMS, a physically based method is used to adjust for size effects in the IEA F82H database and we assess the agreement of the adjusted data with a single MC.

* Corresponding author. Tel.: +1-805 893 3525; fax: +1-805 893 8651.
E-mail address: odette@engineering.ucsb.edu (G.R. Odette).

0022-3115/$ - see front matter © 2004 Elsevier B.V. All rights reserved.
doi:10.1016/j.jnucmat.2004.04.255

2. Background, master curve and specimen size and geometry effects on fracture toughness

Various MC methods *assume* there is a universal invariant toughness temperature curve shape, $K_{Jc}(T - T_0)$, or small family of shapes, in the cleavage transition regime that can be indexed on an absolute temperature (T) scale by a reference temperature (T_0) at a median reference toughness of 100 MPa $\sqrt{m}$ [1–4]. The American society for testing and materials (ASTM) E1921 Standard MC is given by [2]

$$K_{Jc}(T - T_0) = 30 + 70[0.019(T - T_0)] \quad (\text{MPa}\sqrt{m}). \quad (1)$$

T_0 can be measured using a relatively small number of relatively small specimens. The Master curve-shifts method [1,3], adjusts the reference T_0 for the alloy in the unirradiated condition with a set of temperature shifts (ΔT_0) to account for the loading rate [1] and embrittlement [1,3,4,6]. The effects of specimen size and geometry can also be treated in terms of a ΔT_0 and adjusted MC shapes [1,3,5]. Large ΔT_0 may control the lifetime of fusion reactor structures. However, the ΔT_0 that accounts for shallow surface cracks in thin-walled structures has a large negative value, thus may mitigate the effects of embrittlement [3].

The various ΔT_0 can be independently measured and modeled. For example, at irradiation temperatures below about 400 °C, the ΔT_0 for embrittlement can be related the irradiation hardening, measured in tensile $(\Delta\sigma_y)$ or microhardness tests [1,4,6]. Further, models that relate $\Delta\sigma_y$ to metallurgical and irradiation variables derived from fits to the large tensile test database can also be used to help model ΔT_0 [1,3,4,6]. Multiscale models can also be used to relate $\Delta\sigma_y$, hence ΔT_0, to irradiation-induced microstructural evolutions, as well as to guide the development of radiation resistant alloys [3].

There is a large and growing body of data on the fracture toughness of TMS in the unirradiated and, to a lesser extent, irradiated conditions. However, these data represent a wide range of test specimen sizes and types [10–14]. Size and specimen geometry are known to influence the measured values of fracture toughness, K_{Jm}. Indeed, fracture toughness is an intrinsic, geometry and size-independent material property, K_{Jr}, only for very restricted reference conditions of a cracked-body (specimen or structure). Thus in order to assess the applicability of the MC method to TMS, it is necessary to properly account for size/geometry effects and to develop methods to transfer the measured K_{Jm} data to the intrinsic property at a reference condition, K_{Jr} [1,3,5–11], as well as to transfer the K_{Jr} to conditions pertinent to a cracked structure [1,3].

Two different size-effects must be considered. Constraint loss (CL) effects occur when the specimen ligament length, b, and/or thickness, B, are no longer small with respect to the dimension of the plastic zone of the crack [1,3,5–11]. Note that the ligament length is defined as $b = W - a$, where a is the crack length and W is the width of the specimen. Tri-axial constraint elevates the normal stress near the crack tip, σ_{22}, to values of 3–5 times σ_y. Any CL lowers σ_{22}, hence, a higher K_{Jm} is needed for cleavage fracture compared to the K_{Jc} for plane strain, deeply cracked specimens, loaded in bending under small-scale yielding (SSY) conditions.

K_{Jm} and K_{Jc} also increase with a decreasing volume of material under the high σ_{22} stress field near a crack tip [2,3,7–9]. This derives from the fact that cleavage occurs when a critical $\sigma_{22} = \sigma^*$ encompasses a sufficient volume of material to cause the formation and propagation of a microcrack from a broken, brittle trigger-particle, like a large grain boundary carbide. The trigger-particles have statistical size and spatial distributions; hence, they act in a way that is similar to a distribution of the strengths of the links in a long chain. Thus, cleavage is a statistical, weakest-link process, and this has two important consequences. The first is that there is an inherently large specimen-to-specimen scatter in K_{Jm} and K_{Jc}. Second, as noted above, K_{Jm} and K_{Jc} increase as the specimen thickness or crack front length, B, hence stressed volume, decreases. We refer to this as the statistical stressed volume (SSV) effect. The stressed volume scales as BK_J^4 under SSY conditions.

In order to decouple the SSV from CL effects, we recently carried out a single-variable experiment on a large matrix of $a/W \approx 0.5$, 3-point bend specimens, with a wide range of B (8–254 mm) and W (6–50 mm) [3,7–9]. The pre-cracked specimens were fabricated from a large plate section of the unused Shoreham A533B reactor pressure vessel. Eight specimens were tested at $T = -91$ °C and a constant loading rate for each B–W combination. The baseline B–W matrix was complemented by a large number of fracture tests using 1 T compact tension and pre-cracked full and sub-sized Charpy specimens, as well as small bend bars with shallow, $a/W \approx 0.2$, pre-cracks. Tensile tests and optical metallography were also carried out to characterize the constitutive properties and basic microstructure of the steel; and the fracture surfaces were characterized by scanning electron microscopy.

The B–W database showed that CL occurs at loading levels well below the current E1921 censoring limit, defined at $M = b\sigma_y E'/K_{Jm}^2 > M_{lim} = 30$ [2]. However, the data also clearly show a SSV effect that is reasonably consistent with the scaling law in E1921 [2],

$$K_{Jr} = (K_{Jc} - K_{J\min})(B/B_r)^{-1/4}. \quad (2)$$

Here B_r is a reference thickness of 25.4 mm. This expression reflects the stressed volume scaling as BK_J^4, modified by the assumption that cleavage only occurs above a minimum $K_{J\min}$, taken as 20 MPa $\sqrt{m}$ in E1921 [2].

The single-variable B–W database was successfully analyzed with calibrated micromechanically based three-dimensional (3D) finite element (FE) CL models [7–9]. The models were used to separate CL and SSV effects. The models compute the theoretical ratio of the large-scale yielding (LSY) to SSY $[K_{lsy}/K_{ssy}]$ levels that produce the same local crack tip stress field conditions. One model was based on a local fracture criterion that assumes that cleavage occurs when the $\sigma_{22} = \sigma^*$ stress contour encompasses a critical average in-plane area, A^*, of the fracture process zone in front of the crack tip. The model was used to evaluate $[K_{lsy}/K_{ssy}]$ for the Shoreham steel constitutive law as a function of B/W, b, σ^*/σ_y and K_{lsy}, where $K_{Jc} = K_{Jm}/[K_{lsy}/K_{ssy}]$ is evaluated at $K_{lsy} = K_{Jm}$. The calibration of σ^* involved fitting a $\sigma^* - A^* K_{Jc}(T)$ model [1,3,4,7–9] to an independent set of high constraint (≈SSY) K_{Jc} data. Eq. (2) was used to adjust K_{Jc} to a reference K_{Jr} for $B = 25.4$ mm. Another approach to evaluating $[K_{lsy}/K_{ssy}]$, based on a self-calibrated Weibull stress statistical model, gave very similar results [9].

The adjusted K_{Jr} for the B–W Shoreham matrix formed a very self-consistent data population with expected statistical properties and a $T_0 = -84 \pm 5$ °C. The adjustment procedure was also applied to the other UCSB Shoreham data, as well as a large set of K_{Jm} data for the same Shoreham plate section reported by Joyce and Tregoning, for a variety of standard specimens tested over a wide range of temperatures [3,8,9]. Remarkably, the entire Shoreham K_{Jr} database (489 data points) was well represented by a single MC with an ASTM E1921 $T_0 = -85 \pm 5$ °C. Of course, the T_0 of the individual subsets of data varied somewhat, but generally fell within the expected statistical distribution and only 22 of the 489 data points fell outside the 5–95% confidence interval.

3. A K_{Jm} database for the IEA heat of F82H and adjustment to K_{Jr}

The CL and SSV method described above were used to adjust the K_{Jm} IEA F82H database that we have assembled, currently composed of 219 data points. The K_{Jm} data represent a wide range of bend bar and compact tension specimen sizes from research programs at UCSB [10,11], ORNL [12], VTT [13] and NRG [14]. Fig. 1 shows the K_{Jm} data that has been only adjusted for SSV size-effects based on Eq. (2) to a reference $B_r = 25.4$ mm, K_{Jmr}, based on the ASTM E1921 standard; but these data have not been adjusted for CL effects. The MC and the 5% and 95% confidence interval curves based on a ASTM E1921 analysis of the K_{Jmr} data, that yielded a $T_0 \approx -119 \pm 3$ °C, are also shown. A large number of data points fall outside the 5% and 95% confidence interval; and at higher temperatures many

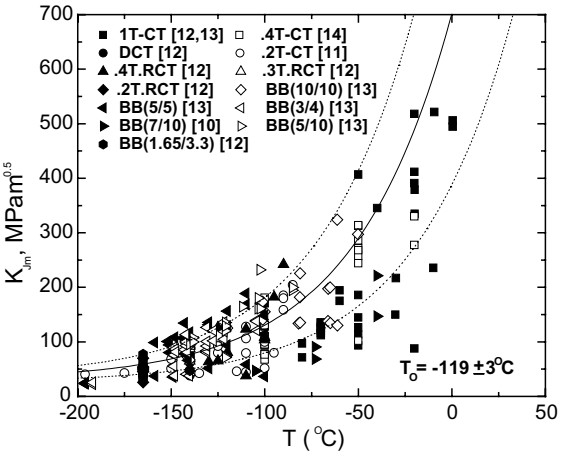

Fig. 1. The F82H K_{Jmr} data versus temperature after a SSV adjustment using Eq. (2) but with no CL adjustment and the median, 5% and 95% confidence interval toughness–temperature curves for the E1921 $T_0 = -119 \pm 3$ °C.

fall below the 5% bound. Thus the K_{Jmr} data are not well represented by a single MC with $T_0 = -119$ °C.

Fig. 2 illustrates the strong effect of CL loss on the IEA F82H database. Here we plot the E1921 T_0 excluding K_{Jm} data with M below a variable censoring limit, M_{lim}, which has a nominal value of 30 in the ASTM Standard. Above $M_{lim} \approx 200$ for the T_0 plateaus at a SSY value of $\approx -98 \pm 5$ °C. However, T_0 decreases below a value of $M_{lim} \approx 200$, at a deformation level that is much lower at the E1921 limit of 30. Thus an E1921 analysis results in a highly non-conservative, small specimen T_0 bias of ≈−21 °C.

The CL adjustment procedure was calibrated to the IEA heat of F82H by fitting the $K_{Jc}(T)$ model to a set of high constraint (≈SSY) data based on a preliminary estimate of $T_0 \approx -94$ °C, [1] yielding $\sigma^* \approx 2100 \pm 100$ MPa for $A^* = 2.5 \times 10^{-8}$ m^2. The CL and SSV adjusted K_{Jr} data are shown in Fig. 3, along with the corresponding MC and the 5% and 95% confidence interval curves based on a multiple-temperature ASTM E1921 analysis that yielded a $T_0 \approx -103° \pm 3$ °C. This is reasonably consistent the best estimate $T_0 = -98 \pm 5$ °C based on the M_{lim} analysis, but reflects a slight residual small specimen bias that will be discussed below.

Fig. 4 plots the differences between the adjusted K_{Jr} data and the MC median toughness, K_{Jo}, as a function of temperature for $T_0 = -98$ °C. The MC 5% and 95%

[1] Note the CL analysis was carried out prior to the multitemperature T_0 evaluation shown in Fig. 3. The preliminary $T_0 = -94$ °C estimate was largely based on the results of data from the largest 1T CT specimens. Re-analysis based on σ^* for a $T_0 = -98$ °C would be possible, but this would not result in a significant change in the conclusions.

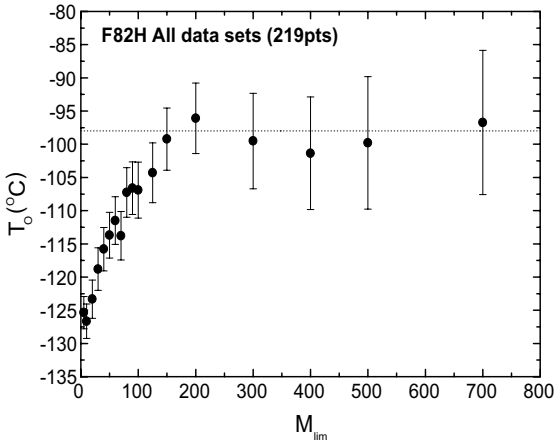

Fig. 2. ASTM E1921 multiple temperature analysis T_0 versus $M_{\lim}$ for the IEA F82H database, showing large effects of constraint loss and a SSY $T_0 \approx -98 \pm 5$ °C at $M_{\lim} > 200$.

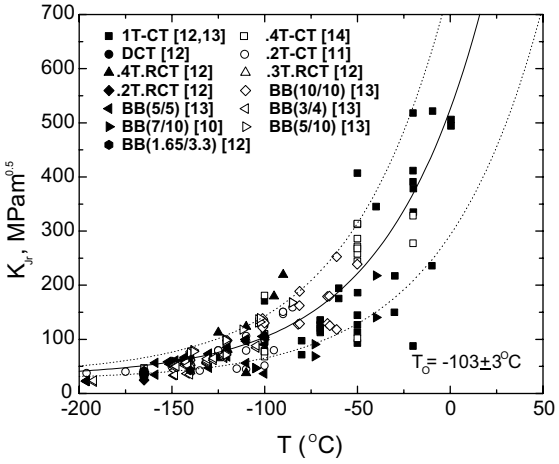

Fig. 3. The F82H K_{Jr} data versus temperature after a SSV and CL adjustment and the median, 5% and 95% confidence interval toughness–temperature curves for the E1921 $T_0 = -103 \pm 3$ °C.

confidence interval curves are also shown, along with average $K_{\mathrm{Jr}} - K_{\mathrm{Jo}}$, and the corresponding standard deviations, in small intervals around common test temperatures. At lower temperatures the adjusted K_{Jr} data are slightly biased to the low side of K_{Jo}. This negative bias decreases at higher temperatures where the data become reasonably well centered, with the average deviations scattering about $K_{\mathrm{Jr}} - K_{\mathrm{Jo}} = 0$. However, a total of 34 data points fall below the nominal 5% and 22 above the 95% confidence interval limits, respectively. This is ≈2.5 times the number (≈22) of data points expected to fall outside the 5–95% confidence interval. However, it is noted that most of these excess deviations are small.

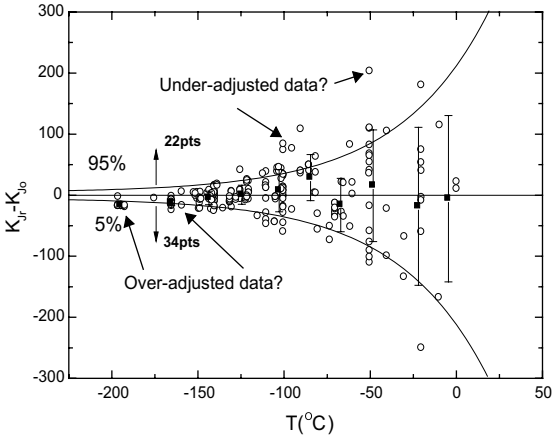

Fig. 4. $K_{\mathrm{Jr}} - K_{\mathrm{Jo}}$ as a function of temperature and the corresponding 5% and 95% confidence interval curves for $T_0 = -98$ °C. The square symbols and error bars are the average and one standard deviation $K_{\mathrm{Jr}} - K_{\mathrm{Jo}}$ for groups of data over small test temperature intervals. The arrows indicate data that may be under-adjusted leading to a slightly lower $T_0 = -103$ °C.

As highlighted by the arrows, examination of Fig. 4 suggests that the CL and SSV model may slightly over-adjust the K_{Jm} data for the very small specimen at low temperature and slightly under-adjust K_{Jm} at higher temperatures, around and above T_0. This leads to a slightly lower $T_0 = -103$ °C for the adjusted K_{Jr} database, compared to the $T_0 = -98$ °C found in the $M_{\lim}$ analysis. This is not surprising, since in bending dominated crack tip fields, the $[K_{\mathrm{lsy}}/K_{\mathrm{ssy}}]$ adjustments are larger at lower σ^*/σ_y. Since σ_y increases with decreasing temperature, σ^*/σ_y decreases. Thus the model may tend to over-adjust the measured data at low temperature and under-adjust at the higher and temperatures. In addition, the applicability of SSV adjustments of low temperature data is questionable; indeed, SSV adjustments of data near or on the lower shelf regime are not recommended in the ASTM E1921 Standard. Further, this assessment assumes that the shape and lower shelf toughness of the MC described by Eq. (1) is precisely applicable to TMS, which may not be the case. Other issues that are not completely resolved relate to the physical basis for and value of $K_{\min} = 20$ MPa $\sqrt{\mathrm{m}}$, and assumptions leading the nominal confidence limits specified in the E1921 Standard. Finally, the excess scatter may in part be due to material heterogeneity for different IEA F82H plate sections and section thicknesses or thickness locations. Such heterogeneity may be have the largest impact on the 25.4 mm CT specimens, with a full though-plate thickness crack, that may sample the lowest toughness microstructure at the center plane. We plan to carry out additional research directly aimed at resolving these issues.

However, the issue of possible excess scatter aside, it is clear that the adjusted K_{Jr} data are in generally good agreement with a single MC with $T_0 = -98 \pm 5$ °C MC. Thus there can be considerable confidence in ΔT_0 evaluations, including for irradiation embrittlement, based on the MC-ΔT method using a sufficient number of small specimens, provided that size effects are properly accounted for. However, assessing the ΔT_0 for irradiation embrittlement raises some additional issues. First, the effect of reduced strain hardening on increased CL in irradiated specimens must be carefully quantified. Second, while results to date are promising [6], the effects of irradiation on the shape of the MC for large $\Delta\sigma_y$ and ΔT_0 are not fully understood.

4. Summary and conclusions

We have assembled a database on the fracture toughness of the IEA heat of F82H. The database, currently composed of 219 data points, is based a wide variety of compact tension and bend bar specimen sizes. An ASTM E1921 evaluation of this database yielded a $T_0 = -119 \pm 3$ °C. However, the data are not well represented by a single MC. In the past, these deviations have raised questions about the applicability of the MC based methods to TMS, or were attributed to material heterogeneity.

However, T_0 is sensitive to the assumed deformation limit, M_{lim}, specified in the E1921 Standard as 30; and T_0 decreases systematically with decreasing M_{lim} starting at a much higher value ≈200 due to constraint loss. At higher $M_{lim} > 200$, T_0 reaches a SSY plateau of $\approx 98 \pm 5$ °C. Thus we applied a calibrated size-adjustment procedure, which accounts for constraint loss effects that are controlled by the specimen size, as well as statistical effects of B. An E1921 analysis of the fully adjusted toughness database gave a $T_0 = 103 \pm 4$ °C, close to the result of the M_{lim} analysis; and the adjusted K_{Jr} data are in reasonably good agreement with a MC with $T_0 = -98$ °C. However, the scatter was somewhat larger than predicted, with ≈25% of the data points falling outside the estimated 5–95% confidence interval. Nevertheless, the excess deviations were generally small and can in part be linked to the approximate adjustment model. The data generally seemed to be slightly over-adjusted at very low temperatures and slightly under-adjusted at temperatures around T_0 and above. Finally, we describe a number of issues that are not fully resolved, including possible excess scatter. However, the results of this study lend strong support to the use of MC-type methods in characterizing the effects of irradiation and other variables on the toughness temperature curves of TMS.

Acknowledgements

This research was supported by the DOE Office of Fusion Energy Science (Grant # DE-FG03-94ER54275). The authors also explicitly acknowledge the large IEA F82H database developed by Dr. K. Wallin of VTT Laboratory in Finland.

References

[1] G.R. Odette, K. Edsinger, G.E. Lucas, E. Donahue, in: Small Specimen Test Techniques, ASTM STP 1329, vol. 3, American Society for Testing and Materials, 1998, p. 298.
[2] ASTM E 1921-03, in: Annual Book of ASTM Standards: Metals Mechanical Testing; Elevated and Low Temperature Tests; Metallography, vol. 3.01, American Society for Testing and Materials, 2003.
[3] G.R. Odette, T. Yamamoto, H.J. Rathbun, M.L. Hribernik, J.W. Rensman, J. Nucl. Mater. 323 (2003) 313.
[4] G.R. Odette, M.Y. He, J. Nucl. Mater. 283–287 (2000) 120.
[5] G.R. Odette, M.Y. He, J. Nucl. Mater. 307–311 (2002) 1624.
[6] G.R. Odette, H.J. Rathbun, J.W. Rensman, F.P. vanden Broek, J. Nucl. Mater. 307–311 (2002) 1011.
[7] H.J. Rathbun, G.R. Odette, M.Y. He, in: Proceedings of the International Congress on Fracture, 10, 2001 (Elsevier CD Format).
[8] H.J. Rathbun, G.R. Odette, M.Y. He, T. Yamamoto, G.E. Lucas, in: Applications of Fracture Mechanics in Failure Assessment, PVP 462, American Society of Mechanical Engineers, 2003, p. 31.
[9] H.J. Rathbun, G.R. Odette, M.Y. He, G.E. Lucas, T. Yamamoto, US Nuclear Regulatory Commission, in press.
[10] P. Spatig, G.R. Odette, E. Donahue, G.E. Lucas, J. Nucl. Mater. 283–287 (2000) 120.
[11] P. Spatig, E. Donahue, G.R. Odette, G.E. Lucas, M. Victoria, in: Multiscale Modeling of Materials 2000, MRS Symposium Proceedings 653, Materials Research Society, 2001, p. Z7.8.
[12] M. Sokolov, R. Klueh, G.R. Odette, K. Shiba, H. Tanaigawa, in: Effects of Irradiation on Materials 21st International Symposium, ASTM STP 1447, American Society for Testing and Materials, in press; private communication.
[13] K. Wallin, A. Laukkanen, S. Tahtinen, in: Small specimen test techniques, V4, ASTM STP, vol. 1418, American Society for Testing and Materials, 2002, p. 33.
[14] J.-W. Rensman et al., J. Nucl. Mater. 307311 (2002) 245.